

Received 21 July 2023, accepted 7 August 2023, date of publication 14 August 2023, date of current version 29 August 2023.

Digital Object Identifier 10.1109/ACCESS.2023.3305252

## RESEARCH ARTICLE

# A Novel FDA-MIMO Deceptive Jamming Method for Neutralizing Phased Array Radar

FAWAD ZAMAN<sup>1</sup>, ZOHAIB AKHTAR<sup>2</sup>, (Senior Member, IEEE), SHAHID MEHMOOD<sup>3</sup>, SADIQ AKBAR<sup>1</sup>, AND GRIDSADA PHANOMCHOENG<sup>1,4,5</sup>

<sup>1</sup>Department of Mechanical Engineering, Chulalongkorn University, Bangkok 10330, Thailand

<sup>2</sup>Department of Electrical and Electronic Engineering, Imperial College London, SW7 2BX London, U.K.

<sup>3</sup>Department of Computer Science and IT, IBADAT International University, Islamabad, Pakistan

<sup>4</sup>Micro/Nano Electromechanical Integrated Device Research Unit, Faculty of Engineering, Chulalongkorn University, Bangkok 10330, Thailand

<sup>5</sup>Applied Medical Virology Research Unit, Chulalongkorn University, Bangkok 10330, Thailand

Corresponding author: Gridsada Phanomchoeng (gridsada.phanomchoeng@gmail.com)


This work was supported by the Second Century Fund (C2F), Chulalongkorn University, Bangkok, Thailand.

**ABSTRACT** Deceptive jamming is one of the indispensable part of electronic countermeasure technology, which has a significant role in modern warfare to secure the aircrafts from imminent threats. This research work proposes a novel Frequency Diverse Array-Multiple Input Multiple Output (FDA-MIMO) deceptive jamming method for neutralizing the opponent Phased Array Radar (PAR). The proposed deceptive jamming model works in passive mode. It interrupts the opponent radar signals and after addition of the deceptive signals, the processed signals are propagated back to neutralize the surveillance operation of the intended radar. When the opponent PAR receives these signals, it perceives multiple fake aircrafts flying at different ranges along the actual aircraft with modified and up-shifted radial velocity. Further, the proposed model uses diversification in frequencies, waveforms, and time modulation to protect the flight of the preferred aircraft. The effectiveness of the proposed model is verified through several simulations in Matlab using different number of arrays, directions and ranges.

**INDEX TERMS** Antenna arrays, electronic warfare, false targets, FDA-MIMO radar, phased array radar, radar deceptive jamming.

## I. INTRODUCTION

Electronic Counter Measure (ECM) techniques are developed to counter the effect of the opponent radar system [1]. Radar deception jamming is an integral part of ECM techniques which plays important role in the field of electronic warfare [2], [3]. It surrenders the effectiveness of the early warning systems (radars) by hiding the desired information of the valuable aircraft, and, on contrarily, providing them false information (false targets, ranges, angles, and radial velocities) about the targets [4], [5], [6], [7]. Hence, it results in total misguidance and confusion in their surveillance operations of the early warning protected shield [8], [9], [10]. Therefore, it is quite difficult for a deployed radar, to retrieve the intended information about the opponent flying target,

The associate editor coordinating the review of this manuscript and approving it for publication was Ravi Kumar Gangwar .

in the existence of the effective radar deception jamming system [11], [12], [13], [14]. Research in radar deception jamming has become center of gravity in the present literature of electronic warfare and ECM technologies [13], [15], [16], [17], [18], [19], [20], [21].

The technique presented in [15] offers an improved method towards the field of radar deception jamming by exploiting scattered waves. Another good contribution is achieved in [16] which generates multiple fake targets by utilizing electromagnetic (EM) wave properties. Radar deception by multiple dummy targets is also obtained by phase-modulation of periodic value  $0-\pi$  in [17]. Further, it assumes a scenario in which the valuable target is accompanied by an escorting drone deceptive jammer flying forward ahead of it. The escorting drone jammer is responsible to secure the flight of the desired target by generating multiple false targets [17]. The method [17] is not appropriate for the fast moving

valuable aircrafts because escorting deceptive drones cannot achieve high flying speeds.

The algorithm presented in [18] uses frequency diverse arrays to offer micro motion deceptive jamming which generates multiple dummy targets having different ranges in the same direction. A novel approach flipped in [19], based on frequency diverse arrays, to confuse opponent radar by displaying him multiple dummy targets with the help of friendly Global Positioning System (GPS). Another research is contributed in [20] which also uses Frequency Diverse Array (FDA) to develop multi- scene deception to misguide the opponent radar, creation of the number of dummy targets is dependent on the length of array elements. A good wave scattering technique is invented in [21] using FDA radar which is exercised to produce multiple fake target deception. A research attempt has been made in [22] to hide to the desired target from the adversary FDA radar using FDA deceiver jammer radar mounted on the actual aircraft. It also generates multiple dummy targets using FDA radar without changing radial velocity of the actual target. Until now, no contribution is taken place in the available literature of radar deception jamming to produce multiple dummy targets and upshifting of radial velocity of the actual target using FDA-MIMO radar against Phased Array Radar (PAR).

This research work proposes a novel Frequency Diverse Array-Multiple Input Multiple Output (FDA-MIMO) deceptive jamming method for neutralizing the opponent PAR. The proposed deceptive jamming model works in passive mode. It interrupts the opponent radar signals and after addition of the deceptive signals, the processed signals are propagated back to neutralize the surveillance operation of the intended radar. When the opponent PAR receives these signals, it perceives multiple fake aircrafts flying at different ranges along the actual aircraft with modified and up-shifted radial velocity. Further, Diversification in waveforms and frequencies of the FDA-MIMO radar are exploited to populate multiple dummy replicas of the actual target and to produce deceptive Doppler shift which turns into increase in radial velocity of the actual target, respectively. The effectiveness of the proposed model is verified through several simulations in Matlab using different number of arrays, directions and ranges.

Salient features of this research work are as follows:

- FDA-MIMO radar is used to produce deceptive jamming against modern PAR.

- Diversification in frequencies is used to up-shift the radial velocity of the desired air craft.

- Diversification in waveforms is exploited to generate multiple dummy aircrafts.

- Time modulation is used to display multiple aircrafts at different ranges along the same directions.

- Mathematical model is designed to verify the effectiveness of the deceptive jamming method.

The remaining part of the research article is structured as:

Section II illustrates data model for the MIMO, FDA, and FDA-MIMO radars, while section III demonstrates the proposed research of radar deception jamming using

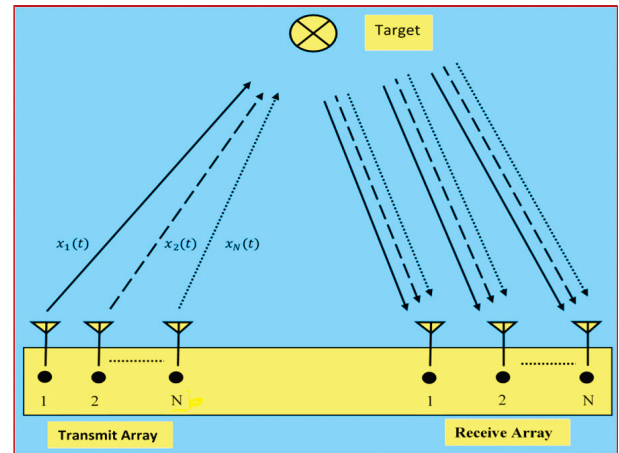


FIGURE 1. Geometry of MIMO radar with N elements.

FDA-MIMO radar against PAR. Section IV explores the effectiveness and validity of the proposed algorithm through multiple simulations considering three different cases. Finally, the conclusion and future directions are given in section V.

## II. DATA MODEL

In this section, we developed data model for the MIMO, FDA, and FDA-MIMO radars.

### A. MIMO RADAR

Multiple Input Multiple Output (MIMO) radar propagates dissimilar signals from each radiating element of the array, thereby it does not make collective beam pattern of Array Factor (AF) [23]. MIMO radars can be categorized into two different types due to physical geometry of the array elements including: spatial diversity (SD) and waveform diversity (WD). If array elements of the MIMO radar are kept at larger distances then it is called SD-MIMO radar; but if array elements are placed closer to each other then it is recognized as WD-MIMO radar. SD-MIMO has better sensing capabilities as independent paths are followed by the propagated signals that fallouts in different fading. But the main constraint upon this type is the cost which comes due to the placement of MIMO systems at different places with larger distances [24]. On the contrast, WD-MIMO radar suitable placement of antenna array elements - kept closer to each other even lesser than a distance of half wavelength [25]. The geometry of MIMO radar with N elements is shown in Fig.1. Array elements of WD-MIMO transmit different waveforms to produce waveform diversity. This type is quite similar to uniform linear arrays (ULA) in terms of spatial arrangements but it is different in waveform generation because, on the contradiction, elements of ULA propagate similar signals. WD-MIMO radar is also known as collocated-MIMO radar. Now assume a collocated-MIMO radar of N identical isotropic radiating elements having equal spacing between the adjacent array-elements can be formulated in

this way [26], [27].

$$s(t) = \sum_{n=1}^N \phi_n(t) \exp\{-j2\pi f_0 t\} \quad (1)$$

where, uniqueness is implanted by the essential form for any time t in the time period T as expressed.

$$\int_0^T \phi_l^*(t - \tau) \phi_k(t) dt = 0, \quad \forall \tau, k \neq l \quad (2)$$

The signal received after some time  $\tau_0$  at any observation point in far-field, can be mathematically given as,

$$s(t, \theta) = \sum_{n=1}^N \phi_n(t - \tau_0) \exp\{-j2\pi f_0(t - \tau_n)\} \quad (3)$$

After putting values for  $\tau_0 = r_0/c$  and  $\tau_n = (r_0 + (n - 1)d \sin\theta)/c$ , we have the following expression,

$$s(t - \tau_0) = \sum_{n=1}^N \phi_n\left(t - \frac{r_0}{c}\right) \exp\left\{-j2\pi \frac{c}{\lambda_0} t + j2\pi \frac{r_0}{\lambda_0} + j2\pi \frac{(n - 1) d \sin\theta}{\lambda_0}\right\} \quad (4)$$

After simple simplification, one can get the final expression for the received signals as follows,

$$s(t - \tau_0) = \exp\left\{j2\pi \left(ct - r_0\right) \frac{1}{\lambda_0}\right\}^* \sum_{n=1}^N \phi_n\left(t - \frac{r_0}{c}\right) \times \exp\left\{j2\pi \frac{(n - 1) d \sin\theta}{\lambda_0}\right\} \quad (5)$$

### B. FDA RADAR

Frequency diverse array (FDA) radar uses diversification of frequencies to get more freedom by getting range dependent radiation pattern, as well as, direction dependent radiation pattern [28], [29], [30]. It feeds array elements with gradual slightly higher frequencies at small increment  $\Delta f$  to each element that provide control over the range dependent radiation pattern [31], [32]. The small frequency increment  $\Delta f$  is normally considered as constant, but it is not necessary. Fig.2, shows an FDA radar having ULA with N isotropic radiating antenna elements. In order to construct mathematical form of the FDA radar, initially, a monochromatic signal is assumed to be propagated from the nth element of FDA radar [33] i.e.,

$$x_n(t) = \exp\{j2\pi f_n t\}, \quad n = 1, 2, 3, \dots, N \quad (6)$$

where,  $f_n = f_0 + (n - 1)\Delta f$  determines frequency of each element, and  $\Delta f$  reflects small constant frequency increment. The transmitted signal, at some far field observation point, after travelling for the time  $\tau_n$ , can be expressed in this way [34], [35]

$$x_n(t - \tau_n) = \exp\{j2\pi f_n(t - \tau_n)\} \quad (7)$$

where,  $\tau_n = \tau_0 - \frac{(n-1)d \sin\theta}{c}$  stands for time taken from the point of transmission to the point of reception,  $\tau_0 = \frac{r_0}{c}$  is the

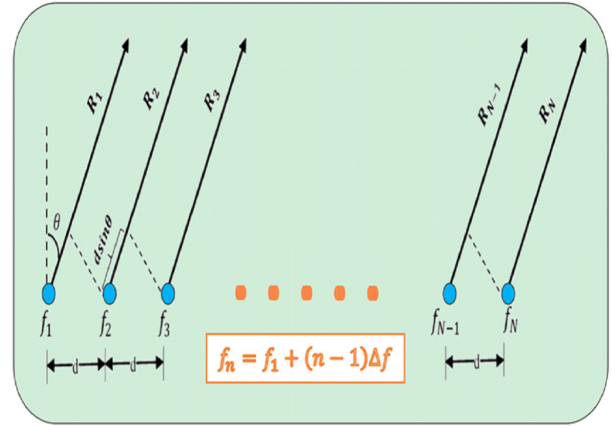


FIGURE 2. Geometry of FDA radar with N elements.

reference time from the reference element to the reception point, and  $r_0$  stands for reference distance from the foremost element of the antenna array to the signal collection point. Moreover,  $d$ ,  $\theta$  and  $c$  represents the inter element separation among the array element, scanning direction, and speed of light, respectively. After incorporating the above values, the Array Factor (AF), for the FDA radar can be mathematically expressed as,

AF

$$= \sum_{n=1}^N \exp\left\{j2\pi [f_0 + (n - 1) \Delta f] \left[t - \frac{r_0 - (n - 1) d \sin\theta}{c}\right]\right\} \quad (8)$$

After doing some basic mathematical steps, the AF in the modified form can be represented as,

AF

$$= \exp\left\{j2\pi \left[f_0 t - \frac{f_0 r_0}{c} + \frac{N - 1}{2} \left(\frac{f_0 d \sin\theta}{c} + \Delta f t - \frac{r_0}{c} \Delta f\right)\right]\right\} \times \frac{\sin\left(\pi N \left[\frac{d \sin\theta}{\lambda_0} + \Delta f t - \frac{r_0}{c} \Delta f\right]\right)}{\sin\left(\pi \left[\frac{d \sin\theta}{\lambda_0} + \Delta f t - \frac{r_0}{c} \Delta f\right]\right)} \quad (9)$$

### C. FDA-MIMO RADAR

In this subsection, we discuss about the unification and combination of both techniques: FDA and MIMO radars [36]. FDA-MIMO radar exploits benefits in diversification of frequency and waveform to get more freedom and detection capabilities [37]. Physical configuration of the FDA-MIMO radar is displayed in Fig.3. To get mathematical expression of FDA-MIMO radar, we consider a linear array of N elements which are placed at equal mutual distances. The transmitted signal from nth element can be given in this way [38].

$$s(t) = \sum_{n=1}^N \phi_n(t) \exp\{-j2\pi f_n t\} \quad (10)$$

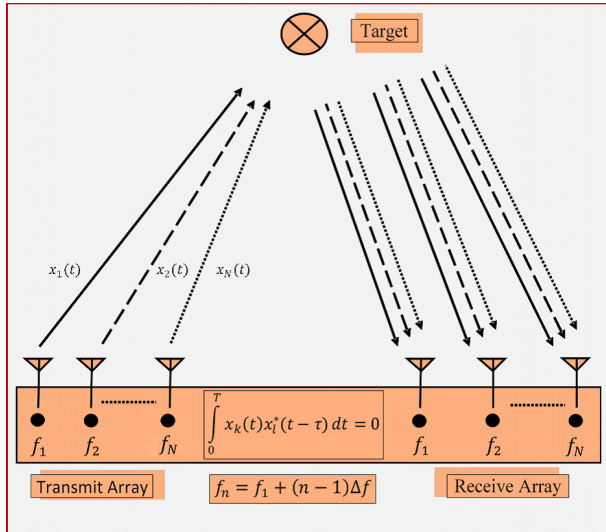


FIGURE 3. Geometry of FDA-MIMO radar with N elements.

The signal, received after passing time  $\tau_0$  and distance  $r_0$  at some point in far-zone field, can be expressed in this way.

$$s(t - \tau_0) = \sum_{n=1}^N \phi_n(t - \tau_0) \exp\{-j2\pi f_n(t - \tau_n)\} \quad (11)$$

After plugging values of  $\tau_n$  and  $f_n$ , the expression can be arranged in this way.

$$s(t - \tau_0) = \exp\left\{j2\pi \left[ct - r_0\right] \frac{1}{\lambda_0}\right\}^* \times \sum_{n=1}^N \left[\phi_n(t - \tau_0) \exp\{j2\pi(n-1)[\psi]\}^*\right] \quad (12)$$

After ignoring the last term due to its insignificance, the final expression can be achieved as,

$$s(t - \tau_0) = \exp\left\{j2\pi \left[ct - r_0\right] \frac{1}{\lambda_0}\right\}^* \sum_{n=1}^N \phi_n(t - \tau_0) \times \exp\left\{j2\pi(n-1)\left(\frac{dsin\theta}{\lambda_0} + \Delta f(t - \tau_0)\right)\right\}^* \quad (13)$$

### III. PROPOSED METHOD

Modern aircrafts are equipped with electronic counter measure (ECM) techniques which pass wrong information about their ranges, directions and velocities to the opponent seeking radar. The evolution of digital radio frequency memory (DRFM) strengthens modern flying carriers to generate fake targets by listening, storing, and transmitting back the received signals to mis-lead the opponent radar.

The proposed deceptive jammer initially works as passive radar; it interrupts opponent radar signals, modify these by adding deceptive Doppler frequency-shift and progressive time-delays, and finally signals are send back towards the

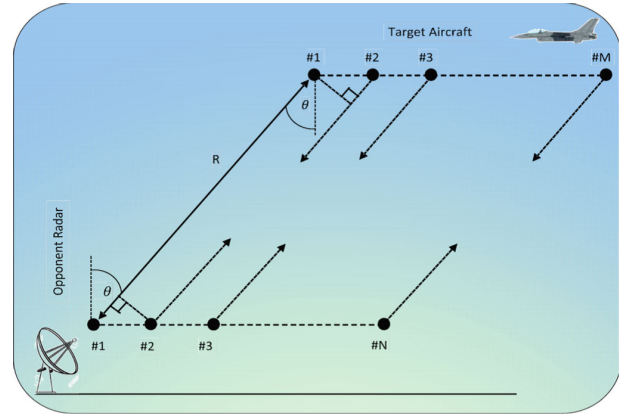


FIGURE 4. Scenario for the proposed deceptive jammer.

opponent radar. The proposed deceptive jammer assumed such a configuration where the FDA-MIMO radar is mounted on the actual aircraft, while PAR configuration is considered on the opponent radar placed at the ground. The proposed scenario is shown in Fig.4. The proposed deceptive technique exhibits multiple false targets having different ranges and velocities due to inclusion of deceptive Doppler shift and progressive time-delays in the intercepted opponent radar signals. PAR with linear array of N elements is assumed as the opponent radar kept on the ground and FDA-MIMO radar is assumed to be mounted on the desired aircraft with linear array of M elements. Both arrays are assumed to be have constant inter-element distance  $d$  for the sake of simplicity. The graphical representation of the anticipated mathematical model is displayed in Fig.4. Suppose the signal is propagated from the  $n^{th}$  element of the opponent PAR, the mathematical expression can be modeled as,

$$x_n = \exp\{j2\pi ft\} \quad (14)$$

where we assume that the actual aircraft is placed at distance  $r$  from the opponent radar. The propagated signal is received by the  $m^{th}$  element of the PAR (in receiving mode),that can mathematically modeled as,

$$y_{m,n} = \exp\{j2\pi f(t - \tau_{m,n})\} \quad (15)$$

where,  $\tau_{m,n} = r - ((n-1)dsin\theta - (m+1)dsin\theta)$  and for the sake of simplicity, the inter-element spacing  $d$  is maintained same and constant in both the radars. In this way, the signals received by the first, second, and  $m^{th}$  elements are expressed as respectively.

$$\begin{aligned} \mathbf{y}_1 &= \left[ e^{j2\pi f(t-\tau_{1,1})} \ e^{j2\pi f(t-\tau_{1,2})} \ \dots \ e^{j2\pi f(t-\tau_{1,N})} \right]_{N \times 1}^T \\ \mathbf{y}_2 &= \left[ e^{j2\pi f(t-\tau_{2,1})} \ e^{j2\pi f(t-\tau_{2,2})} \ \dots \ e^{j2\pi f(t-\tau_{2,N})} \right]_{N \times 1}^T \\ &\vdots \\ \mathbf{y}_M &= \left[ e^{j2\pi f(t-\tau_{M,1})} \ e^{j2\pi f(t-\tau_{M,2})} \ \dots \ e^{j2\pi f(t-\tau_{M,N})} \right]_{N \times 1}^T \end{aligned} \quad (16)$$

Further, it can be stated in matrix form in this way.

$$\mathbf{Y} = [\mathbf{y}_1 \quad \mathbf{y}_2, \dots, \mathbf{y}_M] \quad (17)$$

In extended compact form, it can be given as,

$$\mathbf{Y} = \begin{bmatrix} e^{j2\pi f(t-\tau_{1,1})} & e^{j2\pi f(t-\tau_{1,2})} & \dots & e^{j2\pi f(t-\tau_{1,N})} \\ e^{j2\pi f(t-\tau_{2,1})} & e^{j2\pi f(t-\tau_{2,2})} & \dots & e^{j2\pi f(t-\tau_{2,N})} \\ \vdots & \vdots & \ddots & \vdots \\ e^{j2\pi f(t-\tau_{M,1})} & e^{j2\pi f(t-\tau_{M,2})} & \dots & e^{j2\pi f(t-\tau_{M,N})} \end{bmatrix}^T \quad (18)$$

The  $\mathbf{Y}$  is a Rank-1 matrix whose proof is provided in Appendix-I. Hence, it can be given in vector-matrix form as,

$$\mathbf{Y} = \mathbf{u}\mathbf{v}^H \quad (19)$$

where, the vectors  $\mathbf{u}$  and  $\mathbf{v}$  represents the steering vectors of the opponent PAR and the target radar respectively,  $\mathbf{u} = [e^{j2\pi f(t-r)} \quad e^{j2\pi f(t-r+d\sin\theta)} \quad \dots \quad e^{j2\pi f(t-r+(N-1)d\sin\theta)}]$  while  $\mathbf{v}^H = [1 \quad e^{j2\pi f(d\sin\theta)} \quad e^{j2\pi f(2d\sin\theta)} \quad \dots \quad e^{j2\pi f(M-1d\sin\theta)}]$ .

The target radar behaves like the PAR in the receiving mode. Consider  $f_{dj}$  is a local adjustable frequency-oscillator, then the time  $\tau_{rpd}$  in the received signal is due to the reception and processing delay by the deceptive jammer, so (19) can be modeled as:

$$\mathbf{Y} = (\mathbf{D}^H \mathbf{u})\mathbf{v}^H = (\mathbf{u}^H \mathbf{D})^H \mathbf{v}^H = [\mathbf{v} (\mathbf{u}^H \mathbf{D})]^H \quad (20)$$

where,  $\mathbf{D} = \exp\{j2\pi f_{dj}(t - \tau_{rpd})\} \times \mathbf{I}_N$  and  $\mathbf{I}_N$  is a matrix of identity elements of order  $N$ . After accumulating all signals, the final radiation pattern is given as below,

$$\mathbf{Y} = \mathbf{q}^T [\mathbf{v} (\mathbf{u}^H \mathbf{D})]^H \mathbf{q} \quad (21)$$

where the vector  $\mathbf{q} = [1 \ 1 \ 1 \dots 1]^T_{N \times 1}$ , For the simplicity, we can show the final received signal in the following way.

$$y_m = \sum_{n=1}^N \exp\{j2\pi f_0(t - \tau_{m,n})\} \times \exp\{-j2\pi f_{dj}(t - \tau_{rpd})\} \quad (22)$$

If  $f_{dj} = f_0$ , then above expression can be re-written as:

$$y_m = \sum_{n=1}^N \exp\{j2\pi f_0(t - \tau_{m,n})\} \times \exp\{-j2\pi f_0(t - \tau_{rpd})\} \quad (23)$$

At this stage, we propagate back the above signal subsequently mixing with the radiation pattern of the FDA-MIMO radar, so we attain the following expression.

$$y'_m = \sum_{n=1}^N \exp\{j2\pi f_0(t - \tau_{m,n})\} \times \exp\{-j2\pi f_0(t - \tau_{rpd})\} \times \phi_n(t - \tau_{dd,n}) \exp\{j2\pi f_n(t - \tau_{dd,n})\} \quad (24)$$

where  $\int_0^T \varphi(t) \varphi_l^*(t - \tau) dt = 0, \forall \tau, \text{ and } k \neq l$  and  $f_{d,n} = f_0 + n\Delta f, \quad n = 1, 2, \dots, N$

Similarly  $\tau_{dd,n} = \tau_0 + 2(n - 1)\Delta\tau_d$  represents progressive deceptive time delay shift and  $\Delta\tau_d$  represents ordinary time delay which can be tuned according to the desired deceptive range delay between the targets. The received signal at  $l^{th}$  element of the opponent radar appears to be in this way.

$$y''_{l,m,n} = \exp\{j2\pi f_0(t - \tau_{m,n} - \tau_{l,m})\} \times \exp\{-j2\pi f_0(t - \tau_{rpd} - \tau_{l,m})\} [\phi_n(t - \tau_{dd,n} - \tau_{l,m})] \times [\exp\{j2\pi f_n[t - \tau_{dd,n} - \tau_{l,m}]\}] \quad (25)$$

After accomplishing matched filtering by  $\exp^*(j2\pi f_0 t)$ , the resulted signal output will become as follows

$$y'''_{l,m,n} = \exp\{j2\pi f_0(t - \tau_{m,n} - \tau_{l,m})\} \times \exp\{-j2\pi f_0(t - \tau_{rpd} - \tau_{l,m})\} \times \exp\{-j2\pi f_0 t\} \times [\phi_n(t - \tau_{dd,n} - \tau_{l,m}) \exp\{j2\pi f_n(t - \tau_{dd,n} - \tau_{l,m})\}] \quad (26)$$

It is understood that forward and backward trip-time is same,  $\tau_{m,n} = \tau_{l,m}$ , the above expression will become as.

$$y'''_{l,m,n} = \exp\{j2\pi f_0(t - 2\tau_{m,n})\} \times \exp\{-j2\pi f_0(t - \tau_{rpd} - \tau_{m,n})\} \times \exp\{-j2\pi f_0 t\} \times [\phi_n(t - \tau_{dd,n} - \tau_{m,n}) \exp\{j2\pi f_n(t - \tau_{dd,n} - \tau_{m,n})\}] \quad (27)$$

After doing some mathematical steps, the expression can be down converted into this form.

$$y'''_{l,m,n} = \exp\{j2\pi f_0(-\tau_{m,n} + \tau_{rpd})\} \times \phi_n(t - \tau_{dd,n} - \tau_{m,n}) \times \exp[j2\pi \{f_n(t - \tau_{dd,n} - \tau_{m,n}) - f_0 t\}] \quad (28)$$

By placing value of  $f_n = f_0 + (n - 1)\Delta f$ , we can get this expression.

$$y'''_{l,m,n} = \exp\{j2\pi f_0(\tau_{rpd} - \tau_{m,n})\} \times \phi_n(t - \tau_{dd,n} - \tau_{m,n}) \times \exp[j2\pi \{(f_0 + (n - 1)\Delta f)(t - \tau_{dd,n} - \tau_{m,n}) - f_0 t\}] \quad (29)$$

The final expression can be documented as follows.

$$y'''_{l,m,n} = \phi_n(t - \tau_{dd,n} - \tau_{m,n}) \times \exp\{j2\pi (lf_0\tau_{rpd} - 2f_0\tau_{m,n} - f_0\tau_{dd,n} + (n - 1)t\Delta f - (n - 1)\Delta f\tau_{dd,n} - (n - 1)\Delta f\tau_{m,n})\} \quad (30)$$

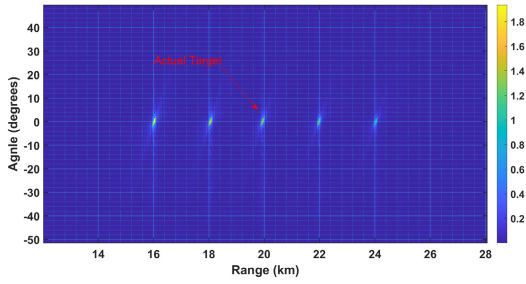


FIGURE 5. Detection of actual along multiple fake targets using 5 elements array.

IV. SIMULATIONS

In this section, several simulations are carried out to verify the validity and effectiveness of the proposed model. The simulation environment is based on the two way model i.e., signals are propagating from the ground surface to the air and then returns back from air to the surface model. The adversary radar is considered to be placed on the ground while the proposed deceptive jammer is mounted on the valuable flying aircraft in the far field to secure its flight. The overall scenario of the assumed model is shown in Fig.4. It is also assumed that the opponent radar has the functionality of PAR system. The proposed deceptive jammer works as a passive searching mode that means it does not transmit probing signals to scan opponent radars, rather it uses impinging signals of the opponent radar for the purpose of deception jamming. Both adversary remote sensors are working in K frequency band (20 GHz) to transmit their electromagnetic signals. The competitor radars are using uniform linear arrays with identical isotropic radiating antenna elements which are spaced equally by half of the carrier communicating wavelength.

For current simulations, it is assumed that the proposed FDA-MIMO based deceptive jammer uses constant frequency increment of 3 KHz among the radiating elements of the array and pulse repetition frequency (PRF) is taken as 5 KHz. Three cases are discussed for varying number of array-elements. The proposed method is verified through two dimensional and three dimensional graphs considering actual target (proposed deceptive jammer) is lying in direction of zero angle with relative to the adversary radar.

1) CASE-I

In this case, array of five elements is considered to secure the valued/desired aircraft located at 20 km away from the opponent radar. The jammer generates four false targets in surrounding of the actual target at different ranges like 16, 18, 22, and 24 km, respectively as shown in Fig.5. Number of achievable dummy false targets are dependent on the array size i.e. for N number of elements in array, one can generate N-1 false targets. Fig.6 shows detection of maximum powers of actual and four false targets at their respective ranges along the same direction. False targets are spread out around the real target having minimum distance of 2 km from each other.

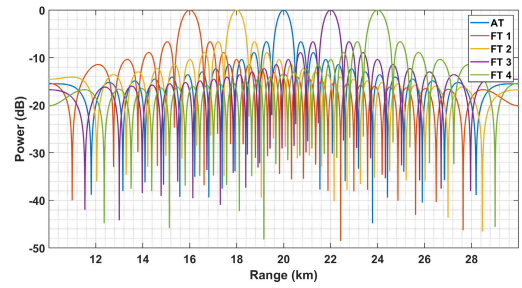


FIGURE 6. Power representation of actual and false targets using 5 elements array.

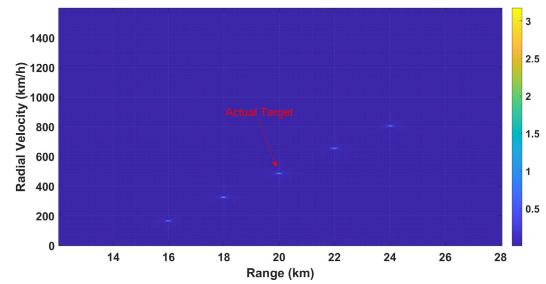


FIGURE 7. Radial velocities of actual and fake targets using array of 5 elements.

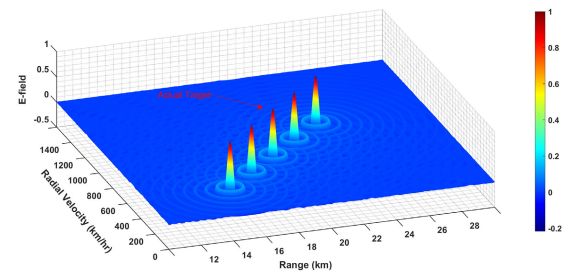


FIGURE 8. 3D visualization of actual and fake targets using array of 5 elements.

The proposed algorithm up-shifts the radial velocities of the actual target as well as of the remaining fake targets that further increase the probability of deception. One can observe from Fig.7, the velocity of the actual target (AT) is up-shifted to 486Km/h. Similarly, the velocities of the fake targets are also changed to 162, 324,648 and 810 Km/h for false target (FT) one, two,three and four respectively. In this way, it will be difficult for the opponent radar to predict the exact futuristic location of the actual flying aircraft due to perturbation of the radial velocity. Fig.8 illustrates the correctness and effectiveness of the offered deception method in three dimension visualization space.

2) CASE-II

For this simulation, FDA-MIMO radar array of six elements is considered to propagate deception towards the opponent radar. It generates five dummy replicas of the actual target having range 20Km. The ranges of the fake targets are 16, 18, 22, 24, and 26 km along the direction of the actual

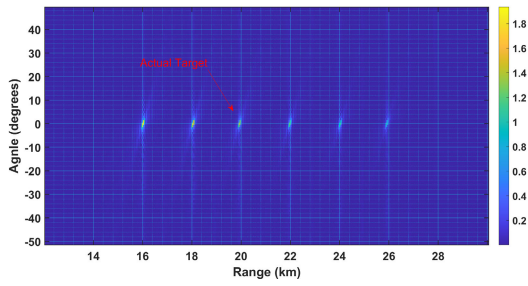


FIGURE 9. Detection of actual target and multiple fake targets using array of 6 elements.

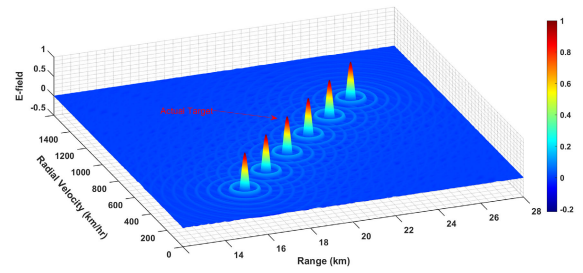


FIGURE 12. 3D visualization of actual and fake targets using array of 6 elements.

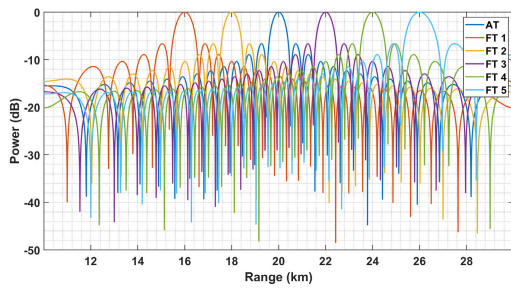


FIGURE 10. Power representation of actual and false targets using array of 6 elements.

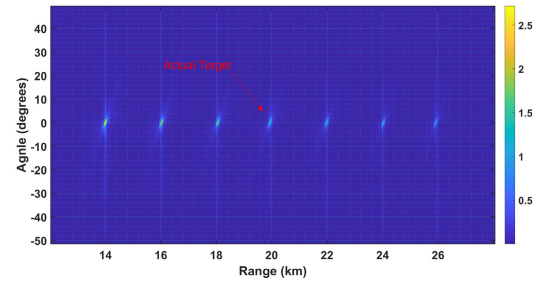


FIGURE 13. Detection of actual target and multiple fake targets using array of 7 elements.

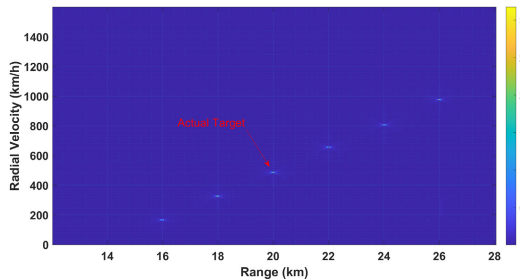


FIGURE 11. Radial velocities of actual and fake targets using array of 6 elements.

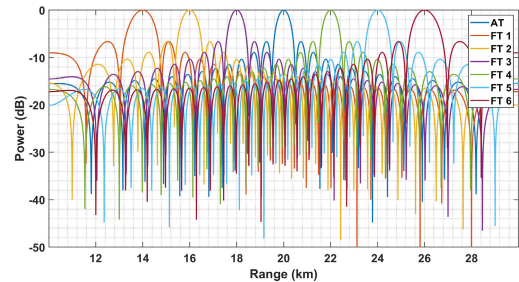


FIGURE 14. Power representation of actual and false targets using array of 7 elements.

target maintaining two kilometer inter-false-target separation as shown in Fig.9.

The proposed algorithm verifies that the opponent perceives delusions by receiving maximum powers at respective assumed ranges of the false targets as depicted in Fig.10. Moreover, radial velocities of the actual and fake targets are respectively up-shifted to 486, 162, 324, 648, 810, 972km/h as shown in Fig.11. Three dimensional visualization of the algorithm is displayed in Fig.12 which further verify the validity of the model.

### 3) CASE-III

In this 3rd case of simulations, we have taken FDA-MIMO array of seven elements to generate six false targets around the actual valuable target at different ranges like 14, 16, 18, 22, 24, and 26 km in the same direction to confuse the opponent radar as shown in Fig.13. The adversary PAR radar detect high powers of the actual and false targets at their

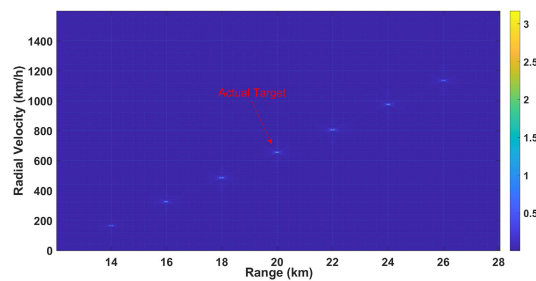


FIGURE 15. Radial velocities of actual and fake targets using array of 7 elements.

intended ranges as depicted in Fig.14. Further, it is evident in Fig.15 that relative radial velocities of the actual and false targets are perturbed efficiently from lower values to higher values that significantly increase the chances of deception. Last simulation of this case reveals three dimensional visualization as shown in Fig.16 which illustrates effectiveness

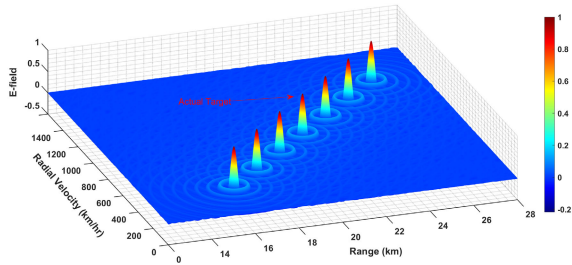


FIGURE 16. 3D visualization of actual and fake targets using array of 7 elements.

TABLE 1. Parameters of actual and false targets.

Case	N	FT	Parameters	AT	FT1	FT2	FT3	FT4	FT5	FT6
1	5	4	Range	20	16	18	22	24	-	-
			Up-shifted radial velocity	486	162	324	648	810	-	-
2	6	5	Range(Km)	20	16	18	22	24	26	-
			Up-shifted radial velocity	486	162	324	648	810	972	-
3	7	6	Range(Km)	20	14	16	18	22	24	26
			Up-shifted radial velocity	648	162	324	486	810	972	1134

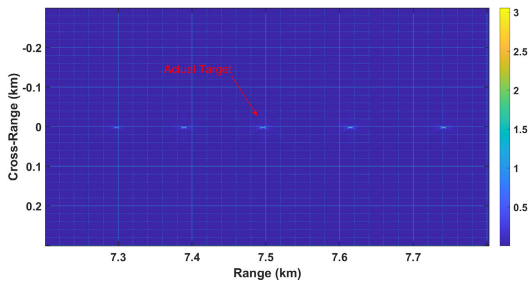


FIGURE 17. Actual target at (7.5, 0) and false targets at (7.3, 0),(7.395, 0),(7.61, 0),(7.75, 0).

and validation of the proposed technique by displaying actual and dummy/fake targets at their corresponding ranges and velocities.

All the above three cases are summarized in Table 1, where N, AT and FT represents the total number of elements, actual target and false targets respectively. All the values of ranges and radial velocities are taken in Km and Km/h respectively.

4) CASE-IV

In this section, comparison of the proposed model is carried out with the techniques discussed in [13], [19], and [21] as shown in Fig.17, 18, and 19. These methods are good contribution to the literature of deception jamming which generate multiple false targets at different ranges. The deceptive technique proposed in [13] produces dummy targets at different ranges but along the same direction of the actual target as shown in Fig.17. The method proposed in [19] produces false targets in different direction relative to the actual target but they are aligned with each other in same direction as shown in Fig.18. In third technique [21], false deceptive targets are

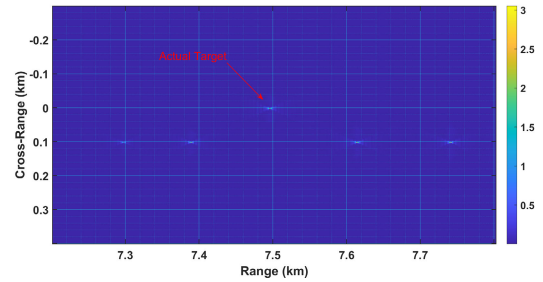


FIGURE 18. Actual target at (7.5, 0) and false targets at (7.3, 0.1),(7.395, 0.1),(7.62, 0.1),(7.75, 0.1).

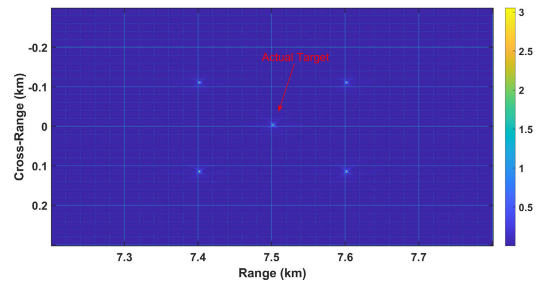


FIGURE 19. Actual target at (7.5, 0) and false targets at (7.4, -0.1),(7.4, 0.1),(7.6, -0.1),(7.6, 0.1).

scattered around the actual target at variable ranges and directions as shown in Fig.19. But none of these techniques are capable of up-shifting the radial velocities of the actual and false targets; and even further they did not use FDA-MIMO radar to produce deception by generating false targets.

V. CONCLUSION AND FUTURE WORK DIRECTIONS

A new algorithm in the field of radar deception jamming has been presented to confuse the opponent PAR by producing multiple false targets and up-shifting the radial velocity of the actual target using FDA-MIMO radar. The FDA-MIMO radar is the combination of frequency diverse array and multiple input multiple output radar which inherits benefits of both the newer technologies that plugins diversification in frequencies and waveforms in radar signals. The algorithm assumed surface to air scenario where the opponent radar was situated at surface while the actual target was flying in the far field.

The proposed model has successfully generate fake targets at fairly enough distance from the the actual target to deceive the opponent radar. Further, the proposed model has also up-shifted the radial velocities of the actual, as well as, of the fake targets that further increase the probability to deceive the opponent radar and hence to protect the flight of the actual aircraft. The limitation of this work is that the proposed model works only against PAR while it does not work against the FDA radar. Further, it is only capable to work with uniform linear arrays rather than working with other famous geometric configurations of antenna arrays. In future, one can address these limitations and further, one can implement the



proposed system through hardware with collaborations of any national or international research organization.

## APPENDIX

The wave travel time from the  $n^{\text{th}}$  element of the opponent radar to the  $m^{\text{th}}$  element of the target is.

$$\tau_{m,n} = r - (n - 1) d \sin\theta + (m - 1) d \sin\theta \quad (31)$$

Elements of the receiving antenna array are as follows.

$$\mathbf{Y} = [\mathbf{y}_1 \mathbf{y}_2 \dots \mathbf{y}_M] \quad (32)$$

Signal received on each element of the target antenna array is shown as.

$$\mathbf{Y} = \begin{bmatrix} e^{j2\pi f(t-\tau_{1,1})} & e^{j2\pi f(t-\tau_{2,1})} & \dots & e^{j2\pi f(t-\tau_{M,1})} \\ e^{j2\pi f(t-\tau_{1,2})} & e^{j2\pi f(t-\tau_{2,2})} & \dots & e^{j2\pi f(t-\tau_{M,2})} \\ \vdots & \vdots & \ddots & \vdots \\ e^{j2\pi f(t-\tau_{1,N})} & e^{j2\pi f(t-\tau_{2,N})} & \dots & e^{j2\pi f(t-\tau_{M,N})} \end{bmatrix} \quad (33)$$

Now we will calculate delay value of each element of the matrix as follows.

$$\tau_{M,N} = r - (N - 1) d \sin\theta + (M - 1) d \sin\theta = r - N d \sin\theta + M d \sin\theta \quad (34)$$

After placing the values of  $\tau$  in the matrix, we get,

$$\mathbf{Y} = \begin{bmatrix} e^{j2\pi f(t-r)} \\ e^{j2\pi f(t-r+d\sin\theta)} \\ \vdots \\ e^{j2\pi f(t-r+(N-1)d\sin\theta)} \end{bmatrix} \begin{bmatrix} 1 \\ e^{-j2\pi f(d\sin\theta)} \\ \vdots \\ e^{-j2\pi f(M-1)d\sin\theta} \end{bmatrix}^T \quad (35)$$

It is evident from the above matrix that it Rank-1 matrix because the factor ( $d\sin\theta$ ) is multiplied with first column to get rest of the columns. All columns except first column of the matrix are dependent, due to this reason the matrix can be recognized as the Rank-1 matrix. It can also be expressed in the simplest form as.

$$\mathbf{Y} = \begin{bmatrix} e^{j2\pi f(t-r)} \\ e^{j2\pi f(t-r+d\sin\theta)} \\ \vdots \\ e^{j2\pi f(t-r+(N-1)d\sin\theta)} \end{bmatrix} \begin{bmatrix} 1 \\ e^{-j2\pi f(d\sin\theta)} \\ \vdots \\ e^{-j2\pi f(M-1)d\sin\theta} \end{bmatrix}^H = \mathbf{u}\mathbf{v}^H \quad (36)$$

where,

$$\mathbf{u} = \begin{bmatrix} e^{j2\pi f(t-r)} & \dots & e^{j2\pi f(t-r+(N-1)d\sin\theta)} \end{bmatrix}^T \quad (37)$$

$$\mathbf{v}^H = \begin{bmatrix} 1 & e^{-j2\pi f(d\sin\theta)} & \dots & e^{-j2\pi f(M-1)d\sin\theta} \end{bmatrix} \quad (38)$$

## ACKNOWLEDGMENT

The authors would like to thank CU VISION X for supporting the hardware and software used in this research and to the Ignite Innovation Laboratory for supporting the research innovation eco-system used.

## REFERENCES

- [1] A. Farina and M. Skolnik, "Electronic counter-countermeasures," in *Radar Handbook*, vol. 2. New York, NY, USA: McGraw-Hill, 2008.
- [2] B. Zohuri and B. Zohuri, "Electronic countermeasure and electronic counter-countermeasure," in *Radar Energy Warfare and the Challenges of Stealth Technology*. 2020, pp. 111–145.
- [3] L. Neng-Jing and Z. Yi-Ting, "A survey of radar ECM and ECCM," *IEEE Trans. Aerosp. Electron. Syst.*, vol. 31, no. 3, pp. 1110–1120, Jul. 1995.
- [4] Y. Liu, W. Wang, X. Pan, D. Dai, and D. Feng, "A frequency-domain three-stage algorithm for active deception jamming against synthetic aperture radar," *IET Radar, Sonar Navigat.*, vol. 8, no. 6, pp. 639–646, Jul. 2014.
- [5] X. Yan, Y. Li, P. Li, and J. Wang, "Multiple time-delay smart deception jamming to pseudo-random code phase modulation fuze," in *Proc. Int. Conf. Comput. Distrib. Control Intell. Environ. Monit.*, Mar. 2012, pp. 428–432.
- [6] P. Shi-Rui, L. Yong-Chun, L. Xin, and D. Wen-Feng, "Study on target pose and deception jamming to ISAR," in *Proc. 2nd Asian-Pacific Conf. Synth. Aperture Radar*, Oct. 2009, pp. 526–530.
- [7] W. Wang, X.-Y. Pan, Y.-C. Liu, D.-J. Feng, and Q.-X. Fu, "Sub-Nyquist sampling jamming against ISAR with compressive sensing," *IEEE Sensors J.*, vol. 14, no. 9, pp. 3131–3136, Sep. 2014.
- [8] Y. Yan-Juan, Z. Feng, A. Xiao-Feng, L. Xiao-Bin, and X. Zhong-Fu, "A study on effectiveness modeling of multi-false-target jamming," in *Proc. CIE Int. Conf. Radar (RADAR)*, Oct. 2016, pp. 1–5.
- [9] Y. Li, G. Lv, and H. Chen, "The study of multi-false targets deception against stepped-frequency waveform inverse synthetic aperture radar," in *Proc. 9th Int. Conf. Signal Process.*, Oct. 2008, pp. 2481–2484.
- [10] B. Rao, Z. Gu, and Y. Nie, "Deception approach to track-to-track radar fusion using noncoherent dual-source jamming," *IEEE Access*, vol. 8, pp. 50843–50858, 2020.
- [11] X.-Y. Pan, W. Wang, and G.-Y. Wang, "Sub-Nyquist sampling jamming against ISAR with CS-based HRRP reconstruction," *IEEE Sensors J.*, vol. 16, no. 6, pp. 1597–1602, Mar. 2016.
- [12] D. Feng, L. Xu, X. Pan, and X. Wang, "Jamming wideband radar using interrupted-sampling repeater," *IEEE Trans. Aerosp. Electron. Syst.*, vol. 53, no. 3, pp. 1341–1354, Jun. 2017.
- [13] Y. Zhu, H. Wang, S. Zhang, Z. Zheng, and W. Wang, "Deceptive jamming on space-borne SAR using frequency diverse array," in *Proc. IEEE Int. Geosci. Remote Sens. Symp. (IGARSS)*, Jul. 2018, pp. 605–608.
- [14] J. Schuenger and D. Garmatyuk, "Deception jamming modeling in radar sensor networks," in *Proc. IEEE Mil. Commun. Conf. (MILCOM)*, Nov. 2008, pp. 1–7.
- [15] B. Zhao, F. Zhou, M. Tao, Z. Zhang, and Z. Bao, "Improved method for synthetic aperture radar scattered wave deception jamming," *IET Radar, Sonar Navigat.*, vol. 8, no. 8, pp. 971–976, Oct. 2014.
- [16] Z. Bo, F. Zhou, X. Shi, Q. Wu, and B. Zheng, "Multiple targets deception jamming against ISAR using electromagnetic properties," *IEEE Sensors J.*, vol. 15, no. 4, pp. 2031–2038, Apr. 2015.
- [17] Q. Shi, C. Wang, J. Huang, and N. Yuan, "Multiple targets deception jamming against ISAR based on periodic  $0-\pi$  phase modulation," *IEEE Access*, vol. 6, pp. 3539–3548, 2018.
- [18] Z. Zong, L. Huang, H. Wang, L. Huang, and Z. Shu, "Micro-motion deception jamming on SAR using frequency diverse array," in *Proc. IEEE Int. Geosci. Remote Sens. Symp. (IGARSS)*, Jul. 2019, pp. 2391–2394.
- [19] W. Mao, H. Wang, S. Zhang, and X. Liu, "A novel deceptive jamming method via frequency diverse array," in *Proc. IEEE Int. Geosci. Remote Sens. Symp. (IGARSS)*, Jul. 2019, pp. 2369–2372.
- [20] H. Wang, S. Zhang, W.-Q. Wang, B. Huang, Z. Zheng, and Z. Lu, "Multi-scene deception jamming on SAR imaging with FDA antenna," *IEEE Access*, vol. 8, pp. 7058–7069, 2020.
- [21] B. Huang, W.-Q. Wang, S. Zhang, H. Wang, R. Gui, and Z. Lu, "A novel approach for spaceborne SAR scattered-wave deception jamming using frequency diverse array," *IEEE Geosci. Remote Sens. Lett.*, vol. 17, no. 9, pp. 1568–1572, Sep. 2020.
- [22] S. Mehmood, A. N. Malik, I. M. Qureshi, M. Z. U. Khan, and F. Zaman, "A novel deceptive jamming approach for hiding actual target and generating false targets," *Wireless Commun. Mobile Comput.*, vol. 2021, pp. 1–20, Apr. 2021.
- [23] E. Fishler, A. Haimovich, R. Blum, D. Chizhik, L. Cimini, and R. Valenzuela, "MIMO radar: An idea whose time has come," in *Proc. IEEE Radar Conf.*, Apr. 2004, pp. 71–78.

- [24] A. M. Haimovich, R. S. Blum, and L. J. Cimini, "MIMO radar with widely separated antennas," *IEEE Signal Process. Mag.*, vol. 25, no. 1, pp. 116–129, Dec. 2008.
- [25] J. Li and P. Stoica, "MIMO radar with colocated antennas," *IEEE Signal Process. Mag.*, vol. 24, no. 5, pp. 106–114, Sep. 2007.
- [26] P. Stoica, J. Li, and Y. Xie, "On probing signal design for MIMO radar," *IEEE Trans. Signal Process.*, vol. 55, no. 8, pp. 4151–4161, Aug. 2007.
- [27] L. Xu, J. Li, and P. Stoica, "Adaptive techniques for MIMO radar," in *Proc. 4th IEEE Workshop Sensor Array Multichannel Signal Process.*, Jul. 2006, pp. 258–262.
- [28] P. Antonik, M. C. Wicks, H. D. Griffiths, and C. J. Baker, "Multi-mission multi-mode waveform diversity," in *Proc. IEEE Conf. Radar*, Apr. 2006, p. 3.
- [29] P. A. C. Wicks, "Method and apparatus for simultaneous synthetic aperture radar and moving target indication," U.S. Patent 7 646 326 B2, Jan. 12, 2010.
- [30] P. Antonik, M. C. Wicks, H. D. Griffiths, and C. J. Baker, "Frequency diverse array radars," in *Proc. IEEE Conf. Radar*, Apr. 2006, p. 3.
- [31] M. Secmen, S. Demir, A. Hizal, and T. Eker, "Frequency diverse array antenna with periodic time modulated pattern in range and angle," in *Proc. IEEE Radar Conf.*, Apr. 2007, pp. 427–430.
- [32] P. Antonik, M. C. Wicks, H. D. Griffiths, and C. J. Baker, "Range-dependent beamforming using element level waveform diversity," in *Proc. Int. Waveform Diversity Design Conf.*, Jan. 2006, pp. 1–6.
- [33] W.-Q. Wang, "Range-angle dependent transmit beampattern synthesis for linear frequency diverse arrays," *IEEE Trans. Antennas Propag.*, vol. 61, no. 8, pp. 4073–4081, Aug. 2013.
- [34] W. Wang, "Overview of frequency diverse array in radar and navigation applications," *IET Radar, Sonar Navigat.*, vol. 10, no. 6, pp. 1001–1012, Jul. 2016.
- [35] W.-Q. Wang, "Frequency diverse array antenna: New opportunities," *IEEE Antennas Propag. Mag.*, vol. 57, no. 2, pp. 145–152, Apr. 2015.
- [36] P. F. Sarmartino, C. J. Baker, and H. D. Griffiths, "Frequency diverse MIMO techniques for radar," *IEEE Trans. Aerosp. Electron. Syst.*, vol. 49, no. 1, pp. 201–222, Jan. 2013.
- [37] Y. Wang, G. Huang, and W. Li, "Transmit beampattern design in range and angle domains for MIMO frequency diverse array radar," *IEEE Antennas Wireless Propag. Lett.*, vol. 16, pp. 1003–1006, 2017.
- [38] W.-Q. Wang, "Phased-MIMO radar with frequency diversity for range-dependent beamforming," *IEEE Sensors J.*, vol. 13, no. 4, pp. 1320–1328, Apr. 2013.



**ZOHAIB AKHTAR** (Senior Member, IEEE) received the B.Sc. degree (Hons.) in electrical engineering and the master's degree in electrical power engineering from the University of Engineering and Technology (UET), Lahore, Pakistan, and the Ph.D. degree in electrical engineering from Imperial College London. The prestigious Commonwealth Scholarship funded him for the Ph.D. studies.

During the master's studies, he was an Erasmus Mundus (EURECA) exchange student with the University of Paderborn, Germany. He is an experienced academic with research and teaching experience of nine years, as a Lecturer/an Assistant Professor, and four years, as a Research Post-Graduate. He was a Postdoctoral Research Associate on multiple projects. He is currently a Senior Teaching Fellow with Imperial College London. He is a Fellow of the Higher Education Academy (FHEA), a Chartered Engineer (CEng) registered with the Engineering Council U.K., and a Professional Engineer registered with Pakistan Engineering Council. He received the Gold Medal from the Prime Minister of Pakistan on the 19th Convocation of UET Lahore, for securing the first position in electrical engineering specialisation in power systems.



**SHAHID MEHMOOD** received the Ph.D. degree in electronic engineering from International Islamic University, Islamabad, Pakistan, in 2023.

Since 2012, he has been with the Department of Electrical Engineering, IBADAT International University, Islamabad, where he is an Assistant Professor. His research interests include FDA-MIMO radar, deceptive jamming, adaptive beamforming, and null steering.



**SADIQ AKBAR** was born in Charsadda, Khyber Pakhtunkhwa, Pakistan. He received the B.Sc. and M.Sc. degrees (Hons.) in electronics, in 1996 and 1998, respectively, the M.S. degree (Hons.) in telecom and networks from Gandhara University, Peshawar, Pakistan, in 2010, and the Ph.D. degree from the University of Peshawar, in 2018. He is currently pursuing the Ph.D. degree with Chulalongkorn University, Thailand.

He has been a Lecturer with the Department of Electronics, since 2000, where he has been an Assistant Professor, since 2010. His research interests include MIMO radars, parameter estimation, system identification, evolutionary computing, swarm intelligence, and optimization methods.



**GRIDSADA PHANOMCHOENG** received the B.S. degree in mechanical engineering from Chulalongkorn University, Bangkok, Thailand, in 2002, and the M.S. degree in aerospace engineering and mechanics and the Ph.D. degree in control science and dynamical systems from the University of Minnesota, Twin Cities, Minneapolis, MN, USA, in 2007 and 2011, respectively.

In 2012, he was a Postdoctoral Researcher with the Dr. Rajamani's Mechanical Engineering Laboratory, University of Minnesota. He is currently a Faculty Member of mechanical engineering with Chulalongkorn University. His research interests include advanced control system design, observer design for nonlinear systems, system identification, applications to automotive systems, energy harvesting, and machine vision.

...



**FAWAD ZAMAN** received the M.S. and Ph.D. degrees in electronic engineering from International Islamic University, Islamabad, in 2009 and 2013, respectively.

Since July 2014, he has been with the Department of Electrical and Computer Engineering, COMSATS University Islamabad (CUI), Pakistan, where he is a tenured Associate Professor. From 2021 to 2022, he was a Postdoctoral Research Fellow with the Department of Electrical and Electronic Engineering, Imperial College London, U.K. He is currently pursuing Postdoctoral research work with Chulalongkorn University, Thailand. He is the author of more than 50 research articles. His research interests include array signal processing, wireless communication, beamforming, direction of arrival estimation, antenna arrays, MIMO radar systems, and optimization techniques. He served as a Program Committee Member, a reviewer, and the Session Chair for several international conferences. He is the Lead Guest Editor of several special issues.